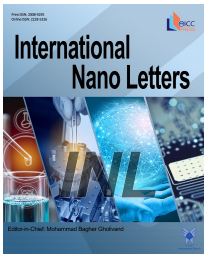

Volume 15, Issue 2, 152506 (1-15)

International Nano Letters (INL)

https://doi.org/10.57647/inl.2025.1502.06

Sonneratia caseolaris-Mediated Silver Nanoparticles: Characterisation and Antibacterial Activity Against *Edwardsiella tarda* from Diseased Freshwater Fish

Alia Syafiqah Aznan[1], Kok Leong Lee[2], Wan Nurhafizah Wan Ibrahim[5], Nur Azna Saari[2], Mohamad Tajuddin Abdul Manaf[2], Norhidayah Mohd Ahyat[3], Ruhil Hayati Hamdan[6], Musa Nadirah[2], Yeong Yik Sung[4], Alyza Azzura Abd Rahman Azmi[3], Faizah Shaharom-Harrison[2], Rossita Shapawi[1], Houjun Pan[7], Musa Najiah[2,*]

[1]*Higher Institution Centre of Excellence, Borneo Marine Research Institute, Universiti Malaysia Sabah, Jalan UMS, Kota Kinabalu, Sabah, Malaysia.*
[2]*Faculty of Fisheries and Food Science, Universiti Malaysia Terengganu, Kuala Nerus, Terengganu, Malaysia.*
[3]*Faculty of Science and Marine Environment, Universiti Malaysia Terengganu, Kuala Nerus, Terengganu, Malaysia.*
[4]*Institute of Climate Adaptation and Marine Biotechnology, Universiti Malaysia Terengganu, Kuala Nerus, Terengganu, Malaysia.*
[5]*Department of Aquaculture, Faculty of Agriculture, Universiti Putra Malaysia, Serdang, Selangor, Malaysia.*
[6]*Faculty of Veterinary Medicine, Universiti Malaysia Kelantan, Pengkalan Chepa, Kota Bharu, Kelantan, Malaysia.*
[7]*Pearl River Fisheries Research Institute, Chinese Academy of Fishery Sciences, Xingyu Road, Xi Liang, Liwan District, Guangzhou, China.*

[*]**Corresponding author:** najiah@umt.edu.my

Original Research

Received:
29 April 2025
Revised:
14 May 2025
Accepted:
2 June 2025
Published in Issue:
30 June 2025

Abstract:

Edwardsiella tarda infection can cause significant economic losses to the aquaculture industry. It causes haemorrhagic septicaemia in freshwater and marine fish, and serious health issues in humans and other animals. The abuse of antibiotics in aquaculture has been linked to the emergence of multidrug-resistant bacteria, and silver nanoparticles (AgNPs) are regarded as a potential therapeutic alternative. This study biosynthesised AgNPs using the methanolic leaf extract of *Sonneratia caseolaris*. A 0.1 mg/ml (H2) extract solution formed AgNPs successfully as indicated by brownish colour change after 24 h incubation and evidenced by UV-Vis spectroscopy. Energy-dispersive X-ray spectroscopy (EDS) revealed silver as the main constituent (84.49%). Transmission electron microscopy (TEM) displayed polydisperse, near-spherical nanoparticles with an average size of 22.3 nm. Fourier transform infrared (FTIR) analysis suggested that several functional groups were involved in SC-AgNPs formation. SC-AgNPs exhibited strong antibacterial activity against 12 *E. tarda* isolates from diseased African catfish and Asian swamp eels, including a β-haemolytic strain (ET10). The minimum inhibitory concentration (MIC) and minimum bactericidal concentration (MBC) were determined to be 2.5 μg/mL. This study suggests that SC-AgNPs has the potential as an alternative to antibiotics to reduce the risk of antibioticresistance in aquaculture.

Keywords: Biosynthesis; Green synthesis; Mangrove apple tree; Methanolic leaf extract; Edwardsiellosis

Cite this article: Aznan, A.S., Lee, K.L., Ibrahim, W.N.W., Saari, N.A., Manaf, M.T.A., Ahyat, N.M., Hamdan, R.H., Nadirah, M., Sung, Y.Y., Azmi, A.A.A.R., Shaharom-Harrison, F., Shapawi, R., Pan, H., Najiah, M. *Sonneratia caseolaris*-Mediated Silver Nanoparticles: Characterisation and Antibacterial Activity Against *Edwardsiella tarda* from Diseased Freshwater Fish. *Int. Nano Lett.* **15**(2), 152506 (2025).

1. Introduction

An *Edwardsiella tarda* infection, known as Edwardsiellosis has been reported globally across a diverse range of hosts, including aquatic animals, mammals, amphibians, and reptiles [1], aquatic birds [2], as well as in humans [3]. *E. tarda* is one of the serious fish pathogens causing significant losses in the aquaculture sector [4]. Fish infected with *E. tarda* exhibit symptoms such as pigmentation, bulging eye (exophthalmia), opacity of the eyes, abdominal swelling, rectal hernia, and petechial haemorrhage in fin and skin [5]. Common internal abnormalities in fish include fluid accumulation in the abdominal cavity (ascites), localised infections or pus-filled areas (abscesses), inflammation of the abdominal lining (peritonitis), as well as congestion in the liver, spleen, and kidneys [6–8]. The disease outbreaks have been reported in various species of aquatic animals worldwide. For instance, it has been reported in Nile tilapia in Egypt [9], Japanese eels in China [10], grass carp in India [11], olive flounder in Korea [12] and barramundi in USA [6] and red hybrid tilapia [13] in Malaysia.

The overuse and misuse of antibiotics in disease treatment have been linked to the emergence of multidrug-resistant bacteria, including in the aquaculture sector [14]. Silver nanoparticles (AgNPs) are regarded as safe and effective alternative antimicrobials for therapeutic applications. Innovative uses of AgNPs are widely adopted in aquaculture for their unique characteristics such as good chemical stability, catalytic, and antibacterial activity [15]. AgNPs are widely used as antimicrobial agent in aquaculture and fisheries due to their multiple mechanisms against bacterial activity, thus helping prevent the development of antibiotic resistance in fish [16]. AgNPs are among the best choices for multiple roles in the medical field due to the characteristics of silver ions and silver-based compounds which are highly potent to microorganisms [17]. Previous studies have shown that AgNPs are good antimicrobial agents against bacteria, viruses, and parasites [18–20].

The biogenic synthesis of AgNPs using plant extracts is considered a form of green synthesis. They are advantageous because they are clean, nontoxic, cost effective, and environmentally acceptable [21]. Plant extracts contain compounds that act as reducing and stabilising agents in the synthesis of the AgNPs [22]. Secondary bioactive metabolites in plant extracts, including aldehydes, proteins, ketones, terpenoids, flavonoids, polyphenols, tannins, polysaccharides, alkaloids and amines can function as reducing agents, converting silver ions to metallic silver. They also can act as capping and stabilising agents [23]. Extracts from various plant species have reportedly been used in the synthesis of AgNPs, including *Moringa oleifera* [24], *Acer oblongifolium* [25], *Cocos nucifera*, *Calotropis gigantea L.*, *Pistacia atlantica*, *Alternanthera dentate*, *Desmodium gangeticum*, *Terminalia cuneata*, *Prosopis farcta* and *Tribulus terrestris* [26].

Mangrove plants are unique in accumulating higher concentrations of bioactive compounds compared to terrestrial plants, owing to their ability to adapt to diverse environmental stresses [27]. Previous studies have reported the presence of diverse bioactive compounds in *S. caseolaris* leaf extracts, including tannins, flavonoids, saponins, alkaloids, steroids, terpenoids, proteins, vitamins, and enzymes [28–30]. It has also been reported as a more potent bioreductant mangrove species than *Sonneratia apetela* and Avicennia alba in green synthesis of AgNPs [31]. Audah et al. [32] further demonstrated that *S. caseolaris* crude extract exhibited higher yield of phenolic compounds and stronger antioxidant activity than mangrove species such as *Avicennia marina*, *Rhizophora mucronate*, and *Rhizophora apiculate*. These bioactive compounds have strong reducing, capping, and stabilizing abilities, underscoring the plant's potential for AgNPs synthesis. In Malaysia, the ecological abundance of *S. caseolaris* in the mangrove forests along the east coast of Peninsular Malaysia provides a sustainable and readily available source for the AgNPs synthesis. However, the limited studies on its use for this purpose have hindered its application in the country.

The present study employed a green synthesis approach for AgNPs using the methanolic leaf extract of *S. caseolaris* (common names: crabapple mangrove, mangrove apple, firefly mangrove). The characteristics of SC-AgNPs were analysed using UV-Vis spectroscopy, Fourier transform infrared spectroscopy (FTIR), scanning electron microscopy-energy dispersive X-ray spectroscopy (SEM-EDS), and transmission electron microscopy (TEM). The antibacterial activities were evaluated against *E. tarda* isolates from diseased freshwater fish.

2. Materials and methods

2.1 Fish samples

Thirty-nine diseased freshwater fish, including African catfish (*Clarias gariepinus*, n = 12), Asian swamp eel (*Monopterus albus*, n = 13), snakehead (*Channa striatus*, n = 4), climbing perch (*Anabus testudineus*, n=5), and red hybrid tilapia (*Oreochromis* spp., n = 5), all exhibiting haemorrhagic and necrotic lesions on their bodies, were collected from the East Coast states of Terengganu (Bukit Tunggal and Chabang Tiga) and Kelantan (Rantau Panjang) in Peninsular Malaysia (West Malaysia) (figure 1).

2.2 Isolation and identification of *E. tarda*

The fish were euthanised under deep anaesthesia induced with Tricane Methanesulfonate (MS222) (Syndel, Canada), and aseptically dissected. The liver, kidney, gill, eye and skin lesions were sampled for bacterial isolation using xylose lysine deoxycholate (XLD) agar (Merck, Germany) with 24 to 48 h incubation at 28 °C. Clear pink colonies measuring 1 to 3 mm in diameter with a black centre on XLD agar, were subcultured onto tryptic soy agar (TSA) (Merck, Germany) to obtain pure cultures for further use and storage. The isolates were characterised by Gram staining, oxidase and indole tests, and haemolysis assay (blood agar) [2], the BBL Crystal Enteric/Nonfermenter (E/NF) Identification System, and 16S ribosomal RNA gene sequence analysis.

DNA was extracted from colony (TSA culture) suspension in TE buffer (500 µL, pH 8.0) in microcentrifuge tubes by boiling technique (100 °C for 15 min, then instantly placed in ice for 15 min) [33]. DNA samples were diluted 1:100 with sterile distilled water, and quantified spectrophotomet-

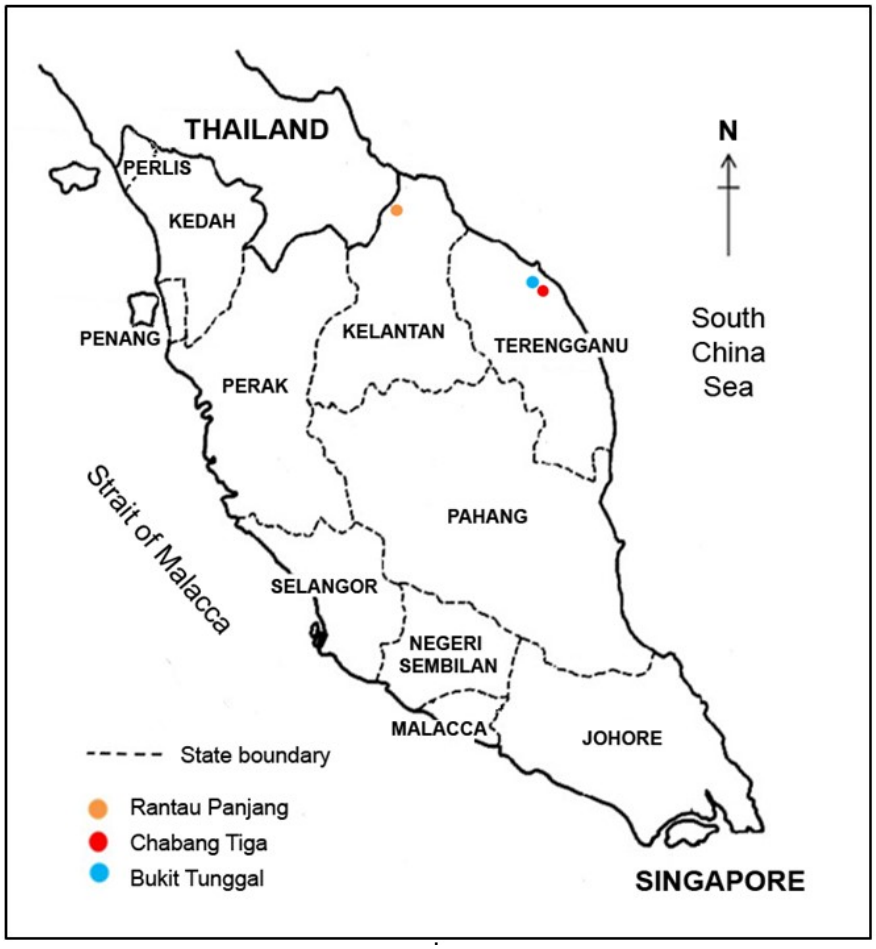

Figure 1. Map of Peninsular Malaysia showing the sampling sites in the east coast states of Terengganu and Kelantan.

rically (260/280). The 16S rRNA gene PCR was conducted as outlined by Nurhafizah et al. [14], using the forward primer fD1 (5′-AGAGTTTGATCCTGGCTCAG-3′) and reverse primer rP2 (5′-ACGGCTACCTTGTTACGACTT-3′) in a reaction volume of 30 µL in a Nexus Gradient Flexlid Master Cycler (Eppendorf, Germany) with the following conditions: 1 cycle at 95 °C for 2 min; 40 cycles at 94 °C for 30 s, 58 °C for 30 s, 72 °C for 1 min 30 s; 72 °C for 7 min final extension, and hold at 10 °C. PCR product (6 µL) was analysed in parallel with 100 bp DNA ladder (Fermentas, Lithuania) by 1.5% agarose gel electrophoresis in 1X TBE buffer at 90V for 60 min. The gel was stained and viewed using UV transilluminator to verify the presence of the 1,500 bp target band. The remaining PCR products were purified using GeneMatrix PCR/DNA Clean-up DNA Purification Kit (EURx, Poland), and subjected to commercial dideoxy chain termination DNA sequencing (First Base, Malaysia). The deduced sequences were processed using BioEdit, and then subjected to NCBI BLAST analysis for taxonomic identification.

2.3 Preparation of *Sonneratia caseolaris* leaf extract

Mangrove apple *S. caseolaris* leaves were collected from the mangrove wetland located near the campus of Universiti Malaysia Terengganu (UMT). The plant species was identified based on plant morphology (the shape and size of the leaves and fruits) by the General Biology Laboratory, UMT. The samples were washed and dried in oven at 50 °C for three days before being grinded into powder. The leaf powder was soaked in 80% methanol (1:10 w/v) for three days. The methanolic extract was then filtered with Whatman filter paper (11 µm), concentrated by rotary evaporation [34], and freeze-dried. The dry extract powder was stored at −20 °C for further use.

2.4 Green synthesis of AgNPs mediated with *S. caseolaris* leaf extract

AgNPs were synthesised based on method presented by Ravichandran et al. [35] with slight modifications. Four reaction mixtures (H1, H2, H3, and H4) were prepared by adding 0.5 mL, 0.1 mL, 0.05 mL, and 0.01 mL of 10 mg/mL *S. caseolaris* leaf extract solution, respectively, to 1 mL of 0.01 M $AgNO_3$ solution. The total volume was adjusted to 10 mL with deionised water in a volumetric flask to yield working extract concentrations of 0.5 mg/mL (H1), 0.1 mg/mL (H2), 0.05 mg/mL (H3), and 0.01 mg/mL (H4), respectively, along with a working concentration of $AgNO_3$ solution at 0.001 M. The reaction mixtures were kept at room temperature (28 ± 0.5 °C) in the dark conditions for 24 h until the brownish colour fully developed, indicating the completion of Ag^+ ion reduction to metallic silver (Ag^0), and the synthesis of SC-AgNPs.

2.5 Characterisation of *S. caseolaris*-mediated silver nanoparticles (SC-AgNPs)

The surface plasmon resonance (SPR) absorption of the prepared brownish SC-AgNPs colloidal solution was observed using a Shimadzu UV-1800 UV/Visible spectrophotometer (Shimadzu, North America) in the range of $380-450$ nm [35]. The colloidal SC-AgNPs was analysed with scanning electron microscope-energy dispersive X-ray spectroscopy (SEM-EDS) (JEOL, Japan) for morphology and elemental composition. Briefly, a drop of the colloidal sample was mounted on the stub, and the sample was dried at room temperature. The stub was then coated with gold, and subjected to SEM-EDS. Transmission electron microscopy (TEM) was used to further determine the size and shape of the colloidal SC-AgNPs. Colloidal samples (10 µL) were loaded onto carbon-coated copper grid, dried at room temperature, and analysed using a JEM-1200 EX TEM at 120 kV (JEOL, Japan). SC-AgNPs were harvested from colloidal solution using centrifugation (5,000 RPM, 15 min). The SC-AgNPs pellet was dried in oven (40 °C, 2 h). Using the dried *S. caseolaris* extract as control for comparison, the dried nanopowder was analysed with Fourier transform infrared spectroscopy (FTIR) to identify the functional groups potentially involved in SC-AgNPs synthesis. The FTIR measurements were carried out using FTIR Spectrum 100 (PerkinElmer, USA) with the KBr pellet technique. The FTIR spectra were collected at a resolution of 4 cm^{-1} in the transmission mode, covering a range of 4000 to 400 cm^{-1}.

2.6 Antibacterial activity analysis

SC-AgNPs were tested for antibacterial activity by well diffusion method against 12 *E. tarda* isolates (ET1-ET12) from diseased freshwater fish. The pure cultures of the bacterial isolates were cultured in tryptic soy broth (TSB) at 35 °C for 24 h. The bacterial suspensions were adjusted to 0.5 McFarland (1.2×10^8 CFU/mL) in 0.85% physiological saline. Wells of 6 mm diameter were made on sterile Muller Hinton agar (MHA) using a sterile cork borer. Each bacterial isolates were spread uniformly onto the individual MHA plates using sterile cotton swabs. 50 µL of SC-AgNPs suspension (resuspended from the dried form of SC-AgNPs using deionised water) was filled into each well of the plates, and the agar plates were incubated at 35 °C for 24 h. Antibiotic discs (Erythromycin 30 µg, E30) were used as a positive control, and *S. caseolaris* leaf extract was used as a negative control. Zone of inhibition measurements were taken following a 24-hour incubation period.

2.7 Minimum inhibitory concentration (MIC) test

The MIC of SC-AgNPs was determined following the method of Krishnan et al. [36] with slight modification using two-fold dilution method in a microtitre plate. SC-AgNPs concentrations ranging from 10 to 0.00125 mg/mL were tested in triplicates. 100 µL of triptic soy broth (TSB) was added into each well of the microtitre plate. 100 µL of SC-AgNPs (10 mg/mL) was then added into the second well and two-fold dilutions were made. Positive growth control was consisted of broth and inoculums (without SC-AgNPs). Following that, 5 µL of the bacterial suspension at 1.2×10^8 CFU/mL (0.5 McFarland turbidity standard) was introduced to the wells. The plates were incubated for 24 h at 32 °C, and observed for turbidity. Microtitre plate with no turbidity was interpreted as negative, whereas the presence of turbidity was interpreted as positive for bacterial growth. Approximately 10 µL of 0.1% 2,3,5-triphenyltetrazolium chloride (TTC) was added into each well and incubated for 1 h at 32 °C, and subsequently observed for colour changes.

2.8 Minimum bactericidal concentration (MBC) test

MBC was determined by sub-culturing 3 µL of the MIC serial dilutions after 24 h of incubation. The bacterial culture was dropped onto Mueller Hinton Agar (MHA) and swabbed with sterile cotton bud, then incubated for 24 h at 28 °C. Bacterial growth was observed and recorded. MBC was determined as the lowest concentration that inhibited the growth of any bacterial colonies on agar medium. The antibacterial activity of SC-AgNPs was measured based on the MBC/MIC ratio. A ratio ≤ 4 is considered bactericidal, while a ratio > 4 is regarded as bacteriostatic [37].

2.9 Statistical analysis

The data of antibacterial assay were presented as mean $\pm$ standard deviation. Independent samples t-tests were performed to compare differences between groups using SPSS® Statistics version 20.0 for Windows®. Exact p-values and 95% confidence intervals (CI) were reported. Each group consisted of three independent replicates ($n = 3$).

3. Results

3.1 Isolation and identification of *E. tarda*

Clinically, although all the diseased fish exhibited haemorrhagic and necrotic lesions (figure 2), *E. tarda* was only successfully isolated from the diseased eels and African catfish. Of the 12 *E. tarda* isolates (ET1-ET12), only isolate ET10 exhibited β-haemolysis on blood agar. Six isolates (50%) were derived from the skin lesions, two (17%) each from the gill lesions and the kidney, one each (8%) from the eye lesion and the liver (Table 1). The biochemical and enzymatic reaction of all isolates were shown in Table 3 (a) and Table 3 (b). All isolates appeared as small ($1-3$ mm) scattered pinkish colonies with black centre on XLD agar plate, and whitish colonies on TSA (figure 3). The 16S rRNA gene PCR amplified target DNA fragment of approximately 1,500 bp from the representative isolate ET10. BLAST analysis of the deduced DNA sequence showed highest similarity (99.78%) with the 16S rRNA gene sequence of *E. tarda* strain C7-5M (HQ663902.1). The sequence of ET10 was deposited into GenBank as KF751244 (http://www.ncbi.nlm.nih.gov/nuccore/KF751244).

3.2 Verification and characterisation of SC-AgNPs

The addition of *S. caseolaris* leaf extract solution to the $AgNO_3$ solution led to a dose-dependent change of colour in the reaction mixtures from light green colour of $AgNO_3$ solution to an increasing density of brownish colour (figure 4), indicating reduction of Ag^+ ions to metallic silver (Ag^0). However, UV-Vis spectroscopy only verified SC-

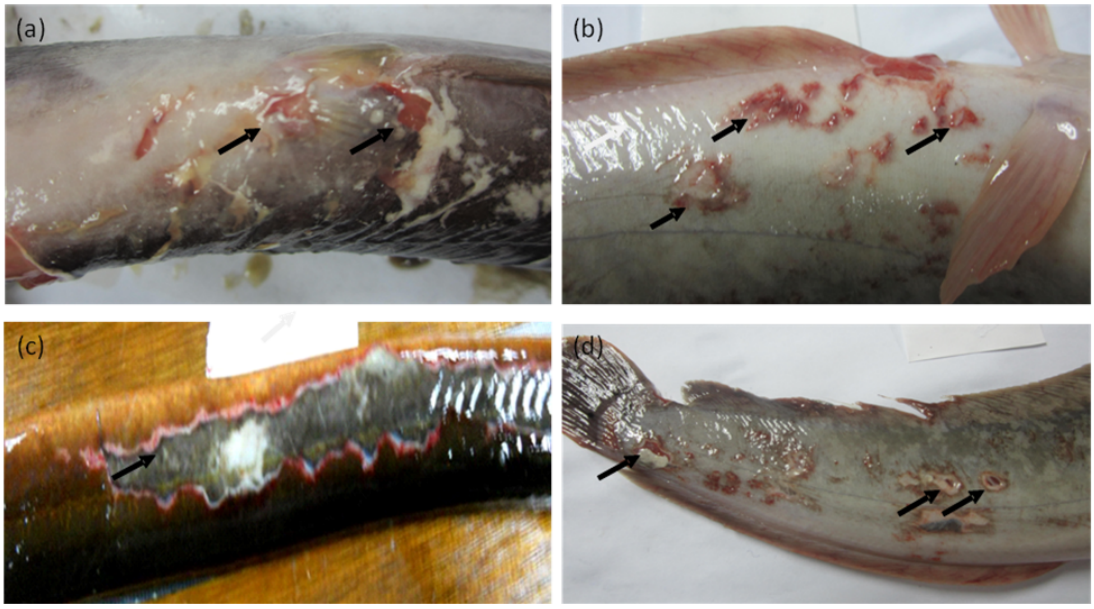

Figure 2. Lesions observed in catfish and eel, (a) Haemorrhagic and necrotic skin lesions in African catfish, (b) multiple focal haemorrhages on the abdomen of African catfish, (c) ulceration on the skin of eel, (d) ulceration on the skin of African catfish.

AgNPs formation in reaction mixture H2 (at an extract concentration of 0.1 mg/mL). Surface plasmon resonance (SPR) screening of AgNP synthesis reaction samples was carried out between 300 and 500 nm after 24 h of reaction. The UV-Vis spectra analysis showed a single and optimum absorbance peak at 424 nm for the H2 sample, and the broadening of peak indicated that the SC-AgNPs were polydisperse (figure 5). Reaction mixtures H1, H3 and H4 did not result in absorbance peak. Thus, sample H2 was used for further analyses of SC-AgNPs.

Table 1. Sources of *E. tarda* isolates and their haemolytic properties.

Isolates	Species	Organ	Origin	Haemolysis
ET 1	African catfish	Skin	Chabang Tiga, Terengganu	α
ET 2	African catfish	Skin	Rantau Panjang, Kelantan	α
ET 3	Eel	Gill	Bukit Tunggal, Terengganu	α
ET 4	Eel	Kidney	Bukit Tunggal, Terengganu	α
ET 5	Eel	Kidney	Bukit Tunggal, Terengganu	α
ET 6	Eel	Liver	Bukit Tunggal, Terengganu	α
ET 7	Eel	Skin	Bukit Tunggal, Terengganu	α
ET 8	Eel	Skin	Bukit Tunggal, Terengganu	α
ET 9	Eel	Gill	Bukit Tunggal, Terengganu	α
ET 10	African catfish	Eye	Bukit Tunggal, Terengganu	β
ET 11	African catfish	Skin	Bukit Tunggal, Terengganu	α
ET 12	Eel	Skin	Bukit Tunggal, Terengganu	α

Keys: (ET) *E. tarda* isolates, (−) negative reaction, (+) positive reaction

Table 2. Functional groups involved in the synthesis of SC-AgNPs.

Frequency (cm^{-1})	Functional group	Molecular motion	Intensity
3381	Alcohol	O-H stretch	Strong
2928	Alkane	C-H stretch	Strong
1615	Aromatic	C=C stretch	Medium-Weak
1441	Aromatic	C=C stretch	Medium-Weak
	Carboxylic acid	O-H bend	Medium
1204	Alcohol	C-O stretch	Strong
1045	Alcohol	C-O stretch	Strong

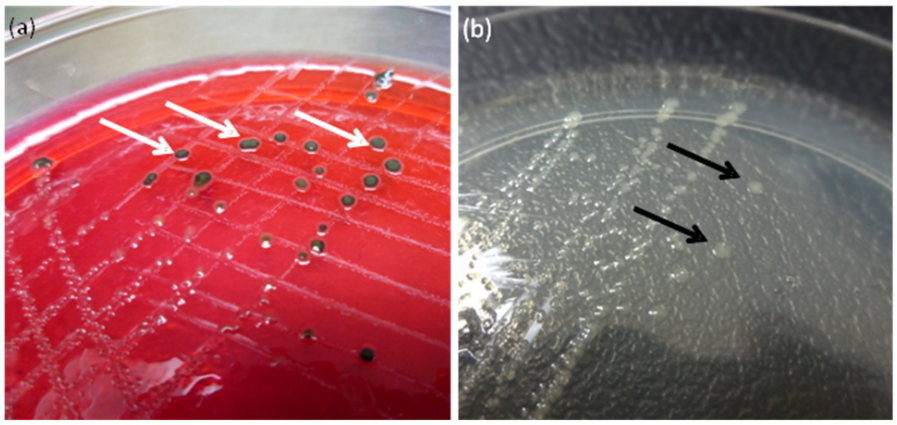

Figure 3. *E. tarda* colonies on (a) XLD and (b) TS agar. (a) The colonies were 1 to 3 mm in size, clear pink with black centre (white arrows); (b) whitish colonies of 1 to 3 mm on TS agar plate (black arrow).

3.3 FTIR spectroscopic analysis

The FTIR analyses of SC leaf extract (control) and SC-AgNPs revealed spectra with peaks at 3381, 2928, 1710, 1615, 1441, 1204 and 1045 cm^{-1} for the control, and 3239, 2932, 1648, 1385, 1202, 1047 and 930 cm^{-1} for SC-AgNPs (figure 6). The functional groups deduced to be involved in the synthesis of SC-AgNPs were shown in Table 2. A peak at 3381 cm^{-1} is a characteristic of the O-H stretch of saponin and tannin groups present in the phytoconstituents. The peaks at 2928 and 1615 cm^{-1} can be assigned to the C-H stretch and C=C stretch, denoting the presence of tannin groups in the *S. caseolaris* extract. The 1441 and 1204 cm^{-1} peaks were attributed to the C=C stretch, O-H bend, and C-O stretch of the phenolic groups in tannin. The peaks at 3381, 1710, 1441, and 1204 cm^{-1} in the control were shifted to lower frequencies at 3239, 1648, 1385, and 1202 cm^{-1}, respectively, in SC-AgNPs, suggesting the involvement of the corresponding functional groups, such as the phenolic group in the extract, in the synthesis of SC-AgNPs.

3.4 SEM-EDS analysis of SC-AgNPs

The EDS profile of SC-AgNPs revealed peaks corresponding to silver (Ag, predominantly Lβ signal at ~ 3.00 keV), oxygen (O, Kα ~ 0.52 keV), fluorine (F, Kα ~ 0.68 keV), and sulfur (S, Kα ~ 2.31 keV and Kβ ~ 2.46 keV). The composition summary indicated that Ag accounted for

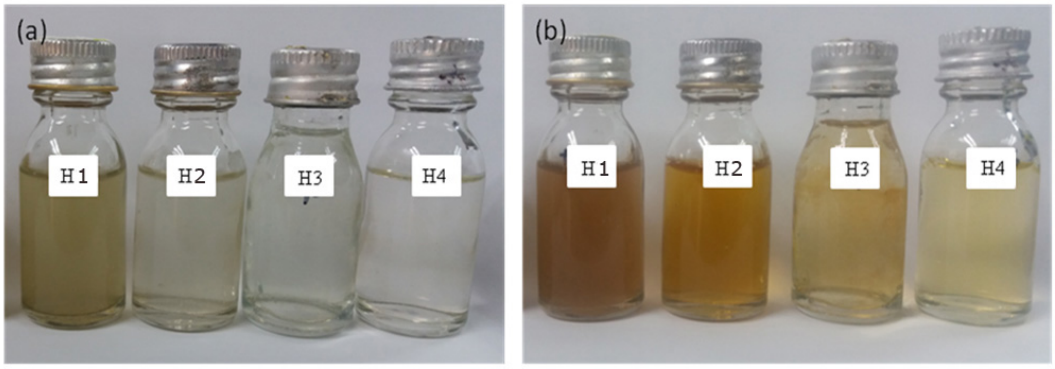

Figure 4. The colour changes to brownish during AgNP synthesis reactions with 0.5 mg/mL (H1), 0.1 mg/mL (H2); 0.05 mg/mL (H3), and 0.01 mg/mL (H4) of *S. caseolaris* extract. (A) zero hour; (B) 24 h.

Table 3. (a) BBL Crystal E/NF biochemical reaction profiles of *E. tarda* isolates.

	ET 1	ET 2	ET 3	ET 4	ET 5	ET 6	ET 7	ET 8	ET 9	ET 10	ET 11	ET 12
Biochemical reaction												
Indole	+	+	+	+	+	+	+	+	+	+	+	+
Oxidase	−	−	−	−	−	−	−	−	−	−	−	−
Arabinose	−	−	−	−	−	−	−	−	−	−	−	−
Mannose	+	+	+	−	+	−	−	+	+	+	+	+
Sucrose	−	−	−	−	−	−	−	−	−	−	−	−
Melibiose	−	−	−	−	−	−	−	−	−	−	−	−
Rhamnose	−	+	−	−	−	−	−	−	−	−	−	−
Sorbitol	−	−	−	−	−	−	−	−	−	−	−	−
Mannitol	−	−	−	−	−	−	−	−	−	−	−	−
Adonitol	−	−	−	−	−	−	−	−	−	−	−	−
Galactose	−	−	−	−	−	−	−	−	−	−	−	−
Inositol	−	−	−	−	−	−	−	−	−	−	−	−
Esculin	−	−	−	−	−	−	−	−	−	−	−	−
p-nitro-DL-phenylalanine	−	−	−	−	−	−	−	−	+	−	−	−
Urea	−	−	−	−	−	−	−	−	+	−	−	−
Glycine	−	−	−	−	−	−	−	−	+	−	−	−
Citrate	−	−	−	−	−	+	+	−	+	+	−	−
Molanate	+	−	−	−	−	−	−	−	−	−	−	−
Tetrazolium	+	−	−	−	−	−	−	−	−	−	−	−
Arginine	−	−	−	−	−	+	+	−	−	−	−	−
Lysine	+	+	+	+	+	+	+	+	+	+	+	+

Keys: (ET) *E. tarda* isolates, (−) negative reaction, (+) positive reaction

Table 3. (b) BBL Crystal E/NF enzymatic reaction profiles of *E. tarda* isolates, and identification confidence level (%).

	ET 1	ET 2	ET 3	ET 4	ET 5	ET 6	ET 7	ET 8	ET 9	ET 10	ET 11	ET 12
Enzymatic reaction												
p-n-p-phosphate	+	+	+	+	+	+	+	+	−	+	+	+
p-n-p-α-β-glucoside	−	−	−	−	−	−	−	−	−	−	−	−
p-n-p-β-galactoside	−	−	−	−	−	−	−	−	−	−	−	−
Proline p-nitroanilide	+	+	+	+	+	+	+	+	+	+	+	+
p-n-p bis phosphate	−	−	−	−	−	−	−	−	−	−	−	−
p-n-p-xyloside	−	−	−	−	−	−	−	−	−	−	−	−
p-n-p-α-arabinoside	−	−	−	−	−	−	−	−	−	−	−	−
p-n-p-phosphorylcholine	−	−	−	−	−	−	−	−	−	−	−	−
p-n-p-β-glucuronide	−	−	−	−	−	−	−	−	−	−	−	−
p-n-p-N-acetyl glucosaminideend	+	+	+	+	+	−	−	+	+	+	+	+
γ-L-glutamyl p-nitroanilide	−	−	−	−	+	−	−	−	−	−	−	−
Confidence value (%)	99.99	99.98	99.99	99.95	99.94	99.58	99.58	99.99	99.99	99.99	99.99	99.99

Keys: (ET) *E. tarda* isolates, (−) negative reaction, (+) positive reaction

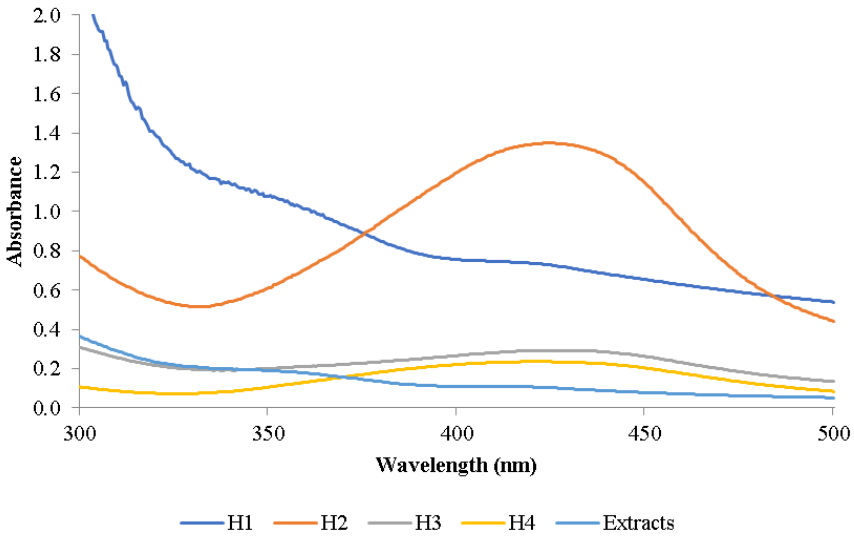

Figure 5. UV-Vis absorption spectra of AgNP synthesis reaction mixtures using different concentrations of *S. caseolaris* extract (H1, 0.5 mg/mL; H2, 0.1 mg/mL; H3, 0.05 mg/mL, H4, 0.01 mg/mL).

most of the nanoparticle weight at 84.49%, followed by O at 11.01%, and F at 4.50%. However, the contribution of S was below the reporting threshold (figure 7).

3.5 TEM analysis of SC-AgNPs

Morphological analysis using TEM showed polydisperse, near-spherical SC-AgNPs (figure 8). Particle size distribution (PSD) analysis showed range from 10 to 40 nm with the average size of 22.3 nm (figure 9).

3.6 Antibacterial activity of SC-AgNPs

The antibacterial activity of SC-AgNPs (H2) was presented in figure 10. The antibacterial effect of SC-AgNPs (H2) on ET1, ET2, ET5, ET8, ET11, and ET12 was higher compared to positive control (E30). An independent sample t-test showed significantly higher antibacterial activity of SC-AgNPs (H2) than E30 against ET4 ($t(2) = -5.00$, $p = 0.038$), with a mean difference of -1.67 (95% CI: -3.10 to -0.23). Significantly higher antibacterial activities of SC-AgNPs (H2) were also observed in ET8 ($t(4) = 3.46$, $p = 0.026$) with a mean difference of 2.00 (95% CI: 0.40 to 3.60), ET11 ($t(2) = 8.00$, $p = 0.015$) with a mean difference of 2.67 (95% CI: 1.23 to 4.10), and ET12 ($t(2) = 5.00$, $p = 0.038$) with a mean difference of 1.67 (95% CI: 0.23 to 3.10). The negative control (SCE) did not produce an inhibition zone, indicating no antibacterial activity against the *E. tarda* isolates. SC-AgNPs produced inhibition zones ranging from 10 to 14 nm in diameter against isolates ET1-ET12, demonstrating variation in their susceptibility to the antibacterial effect. The highest antibacterial effect of SC-AgNPs was recorded against isolate ET10 (14 nm) while the lowest was on isolate ET6 (10 nm).

3.7 MIC and MBC values

The antibacterial effectiveness of SC-AgNPs was assessed by MIC and MBC tests against isolate ET10, which was presumed to be most virulent on the basis β-haemolytic property. The MIC and MBC values were determined to

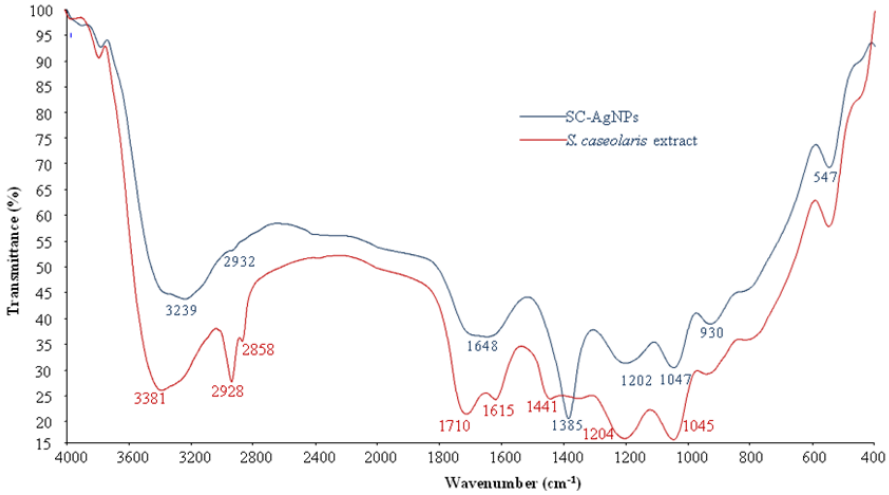

Figure 6. FTIR spectra of *S. caseolaris* extract and SC-AgNPs tracked the chemical changes during SC-AgNPs formation.

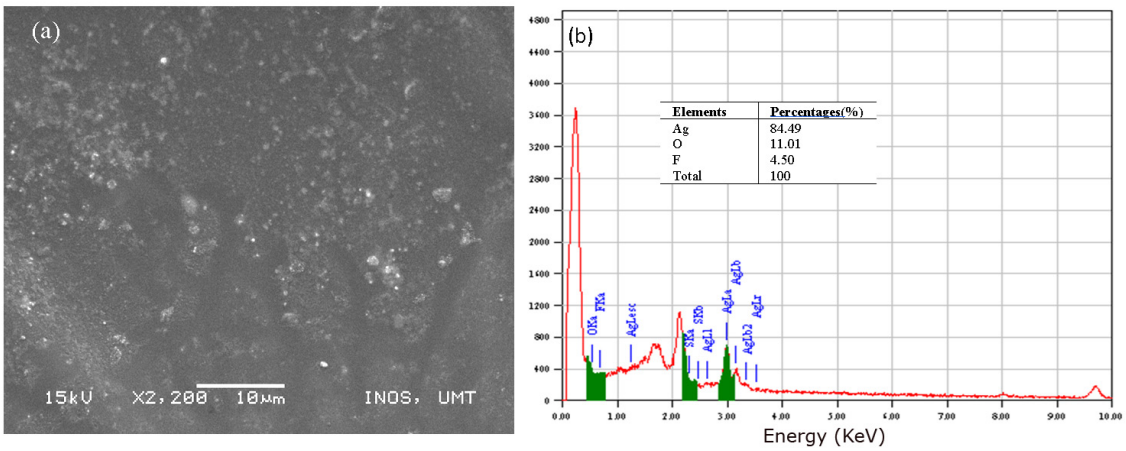

Figure 7. (a) SEM image and (b) EDS spectrum (elemental analysis) of SC-AgNPs. The EDS spectrum shows signals corresponding to Ag (mainly Lβ peak ∼ 3.00 keV), O (Kα peak ∼ 0.52 keV), F (Kα peak ∼ 0.68 keV), and S (Kα peak ∼ 2.31 keV, Kβ peak ∼ 2.46 keV). The composition summary shows that Ag constitutes the bulk of the nanoparticle's weight at 84.49%, followed by O at 11.01%, and F at 4.50%. S is below the composition reporting threshold.

be 2.5 μg/mL. No growth of isolate ET10 was observed on MHA at 2.5 µg/mL and higher concentrations of SC-AgNPs (figure 11). The antibacterial effect was considered to be bactericidal on ET10 because the MBC/MIC ratio was 1.

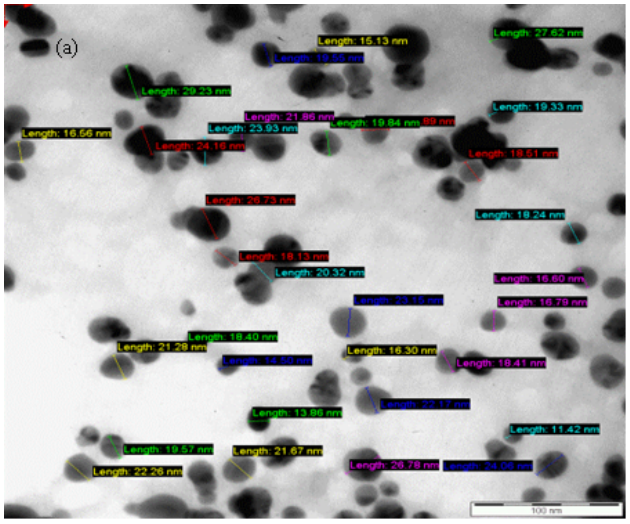

Figure 8. TEM images of near-spherical SC-AgNPs, and particle size distribution (PSD) analysis.

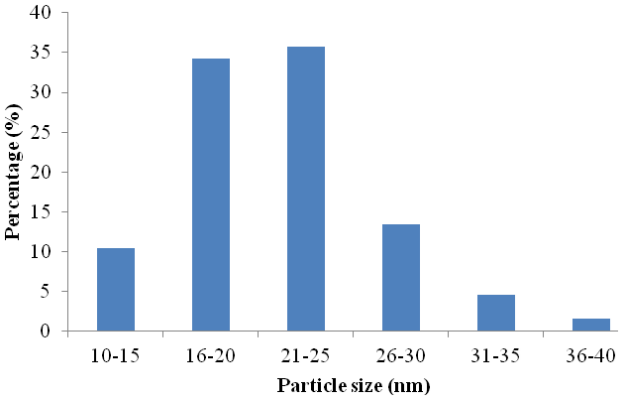

Figure 9. SC-AgNP size distribution ranges from 10 to 40 nm, with an average size of 22.3 nm.

4. Discussion

Edwardsiellosis is among the serious infectious diseases in the aquaculture sector. It can significantly affect the quality, growth performance, and survival rate of the fish. In the present study, *E. tarda* infected fish exhibited haemorrhagic, ulcerative, and necrotic lesions on the skin. Previous study by Park et al. [10] reported hernia, exophthalmia, ascites, haemorrhages and severe lesions in the internal organs of *E. tarda*-infected fish. According to Goh et al. [38], fish infected with *E. tarda* showed loss of pigmentation, skin haemorrhages, exopthalmia, haemorrhagic ascites, and congestion in the liver, spleen, and kidney. In the present study, 50% of *E. tarda* isolates were obtained from the skin lesions of the fish. According to Rediet et al., [5], *E. tarda* are most prone to invading the abraded skin and intestine of the fish. In contrast, Butar-butar et al. [39] found that the highest isolation of *E. tarda* is from kidney, which probably due to poor water quality and high organic content in the water, that disrupted the normal physiological functions of the fish kidney. In the current study, the β-haemolytic strain ET10 is generally regarded as virulent, given its ability to lyse the red blood cells. Haemolysin, the pore-forming toxin, is one of the virulence factors of bacteria alongside adhesion factors, biofilm formation, motility and exoenzymes such as proteases, deoxyribonucleases (DNase), and lipase [40]. In the present study, the brownish colour appearance in the *S. caseolaris* extract and silver nitrate ($AgNO_3$) aqueous solution mixture during incubation indicated successful reduction of silver ions (Ag^+) to metallic silver (Ag^0) by the reducing agents in the extract. This phenomenon of colour change is called surface plasmon resonance (SPR), and occurs due to the excitation of surface plasmon vibrations (quantum oscillations of the free electrons) in silver nanoparticles [41], suggesting an ongoing process of AgNPs formation. The colour change will stop when all the

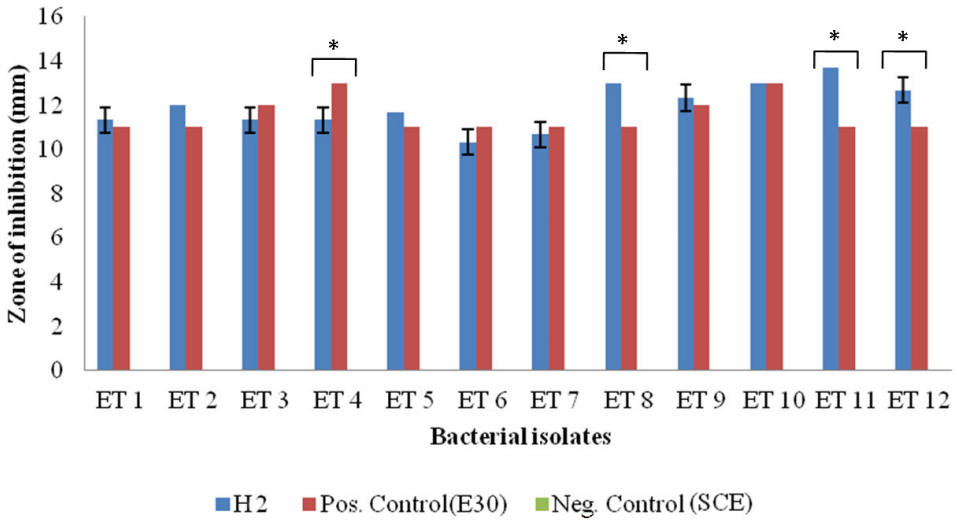

Figure 10. Antibacterial activity of SC-AgNPs (H2) against 12 *E. tarda* isolates. Data was expressed as mean ± SD. *P< 0.05.

Ag^+ ions or reducing agents present are exhausted. The bio-molecule content in the plant extract, and its concentrations are responsible for the extent of colour changes and reduction of Ag^+ ions [42]. Similar findings were reported by using different plant extract include *Malachra capitata (L.)* leaf extract, *Avicennia marina* extract and *Eugenia roxburghii* extract [43–45].

However, despite the reduction of Ag^+ ions in all four reaction mixtures in the present study, successful synthesis of SC-AgNPs was only confirmed in reaction mixture H2 by UV-Vis analysis, which demonstrated an absorption peak at 424 nm. This agrees with Abd El-Aziz and Yousef [46], who stated that the characteristic peaks of the absorption spectra of AgNPs range between $350-550$ nm. According to Vijayaraj et al. [43], the occurrence of absorption peak is due to the excitation of plasmon vibrations on the outer surface of the AgNPs by the applied electromagnetic field. In addition, the current study also demonstrated that SC-AgNPs, with an absorption peak at 424 nm were stable, and well-dispersed without aggregation. Similarly, the AgNPs synthesised using mangrove *Avicennia marina* extract [44] and rosemary extracts [46] exhibited SPR at 420 nm. In the study by Asif et al. [47], AgNPs synthesised using *Moringa oleifera* extracts recorded an SPR peak around 419 nm. In the present study, UV-Vis spectroscopy revealed unsuccessful SC-AgNPs formation in reaction mixtures H1, H3, and H4, despite the successful conversion of Ag^+ ions to Ag^0. The formation likely failed during the stabilisation or cap-

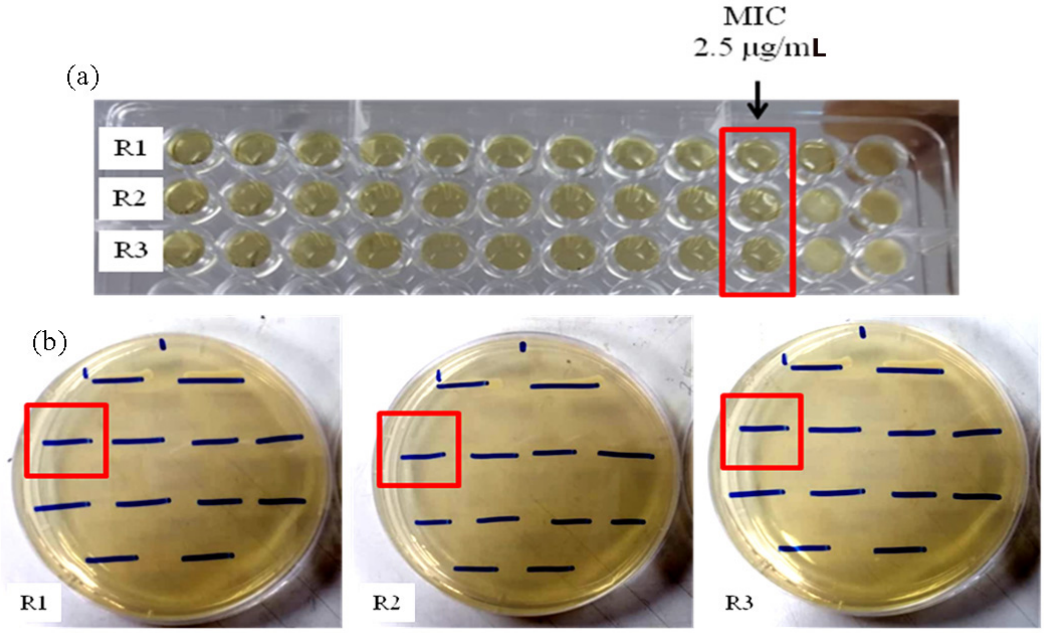

Figure 11. (a) No bacterial growth in the well at a concentration of 2.5 μg/mL. (b) No bacterial growth on the MH agar at 2.5 μg/mL (red box).

ping process due to suboptimal concentrations of stabilising or capping agents in the extract. The low and high concentrations of *S. caseolaris* leaf extract can cause failure in AgNP synthesis [48]. The present study demonstrated that 0.1 mg/mL *S. caseolaris* leaf extract in 0.001 M of $AgNO_3$ aqueous solution is optimal for SC-AgNP formation.

FTIR is an advanced technique for analysing the involvement of phytochemical functional groups, including flavonoids, terpenoids, alkaloids, phenolic acids, and proteins in the reduction and stabilisation processes of AgNP synthesis [49]. In this study, FTIR analysis showed the presence of various organic functional groups in the *S. caseolaris* leaf extract. The functional compounds in the plant extract collectively play reduction, capping and stabilisation roles during AgNP synthesis [50]. In the present study, tannins and steroids likely acted as reducing agents, while saponins and other possible oxygen-containing compounds stabilised the SC-AgNPs. According to Nguyen et al. [51], compounds containing oxygen such as saponins, tannins, and phenolics act as potential capping and stabilising agents for nanoparticles. It also agrees with El-seedi et al. [52], that the functional groups from diverse metabolites of plant extracts react with metal ions, and reduce them to metallic nanoparticles. Jeyapaul et al. [53] have also reported that nanoparticles synthesised using plant extract were surrounded by a thin layer of organic compounds from the extracts, which acted to cap and stabilise the nanoparticles. In the present study, the EDS profiling detected signals corresponding to Ag (primarily at ~ 3.00 keV), O (~ 0.52 keV), F (~ 0.68 keV), and S (~ 2.31 and ~ 2.46 keV), and deduced a composition of 84.49% Ag, 11.01% O, and 4.50% F for SC-AgNP, with S falling below the reporting threshold. The findings strongly support the formation of SC-AgNPs. The finding agrees with Yu et al. [54], who also reported X-ray emission signal of approximately 3 keV for AgNPs. On the other hand, AgNPs synthesised using *M. capitata (L.)* exhibited EDX spectra showing 70.36% Ag at 3 keV [43]. The EDS pattern in the present study did not show any signal for nitrogen (N), suggesting the absence of detectable trace of nitrogen ions from the initially used $AgNO_3$, which is supported by the findings of Kambale et al. [55]. According to Das et al. [56], the presence of oxygen and fluorine is possibly derived from the environment and plant extract, respectively. Kambale et al. [55] suggested that the presence of oxygen atoms in the AgNPs sample is indicative of the existence of organic compounds on the surface of the AgNPs.

The formation of polydisperse near-spherical nanoparticles of $10-40$ nm in the present study agrees with the findings of Hassan and Mustafa [57], due to the presence of diverse reducing, capping and stabilising agents. According to Higo et al. [58], the formation of polydisperse AgNPs, with a layer of the organic material surrounding the AgNPs will result in good dispersion of the nanoparticles in solution. In the current study, nanoparticles in the size range of $21-25$ nm constituted the highest percentage (36%), while those in the $36-40$ nm range accounted for the lowest (2%). Khalandi et al., [59] revealed that the size of AgNPs plays an important role in their antimicrobial activity. This is supported by Dakal et al. [60], who classified AgNPs with sizes less than 50 nm as effective antimicrobial agents. In a previous research by Khalandi et al., [59], AgNPs in the size range of $25-30$ nm exhibited more potent biocidal activity compared to those in the range of $35-52$ nm. The high percentage of small-sized particles ($21-25$ nm) in the SC-AgNPs synthesised suggests their strong potential as effective antibacterial agents.

The SC-AgNPs synthesised in the present study inhibited the growth of all 12 *E. tarda* isolates, with most of them producing a larger inhibition zone than the positive control (Erythromycin 30 µg), indicating strong antibacterial activity against *E. tarda*. The significant antibacterial activity against *E. tarda* may be attributed to the antibacterial property of silver and the small size of SC-AgNPs (average 22.3 nm), and the synergistic antibacterial effects of fluorine, sulfur, and phytobioactive compounds coating the AgNPs as a layer of capping agents. In comparison with chemically synthesised AgNPs, Ibrahim et al. [61] had reported that green synthesis of AgNPs using pomegranate extract exhibit higher antibacterial activity compared with chemically synthesised AgNPs, possibly due to the faster rate of nanoparticle stabilisation mechanism by organic compounds in the extract. Bahraminezhad et al. [62] also reported that green synthesised AgNPs using *Abrimonia eupatoria L.* extract demonstrated significant antibacterial activity against *Escherichia coli* compared with chemically synthesised AgNPs. The smaller size of AgNPs provides a larger contact surface with bacteria, thus increasing their effectiveness in causing bacterial death [59]. This agrees with the findings of Salahuddin et al. [63], who found that small-sized AgNPs are excellent growth inhibitors for bacteria.

The actual antibacterial mechanisms of AgNPs are, however, still controversial. More et al. [64] reported that AgNPs can cause oxidative stress, protein dysfunction, cell membrane disruption and DNA damage which lead to bacterial cell death. According to Roy et al. [65], AgNPs attach to the microbial cell wall and membrane due to the electrostatic attraction between the negatively charged microbial cell membrane and positively charged AgNPs. The morphological changes in the membrane structure triggered by the nanoparticles lead to disruption of membrane permeability and respiratory functions via membrane depolarisation. The infiltration of AgNPs into the bacterial cells causes enzyme inactivation, protein denaturation, DNA damage and ribosome disassembly. As a consequence of increased membrane permeability and cell wall disruption, cellular contents including enzymes, proteins, ions, DNA, metabolites and energy reservoir leak into the environment, ultimately leading to loss of cell integrity and cell death. Therefore, the primary antibacterial mechanism of AgNPs is the disintegration of the cell wall by the nanoparticles' adhesion.

Siddiqi et al. [66] has proved the association between AgNPs and microbial cells with scanning and transmission electron microscopy (SEM and TEM) analyses. TEM revealed cell wall disruption and numerous electron-dense pits at sites of AgNP-induced damage. The strong interaction between ionic Ag^+ and thiol groups of cysteine residues

of protein in the cell wall is one of the mechanisms by which the Ag^+ permeated the cell wall [67]. Girma et. al. [67] reported that the toxic effects of Ag^+ cause the increase in cellular oxidative stress in microbes. The ability of AgNPs to generate reactive oxygen species (ROS) and free radicals including hydrogen peroxide (H_2O_2), superoxide anion (O_2^-), hydroxyl radical ($OH^\bullet$), hypochlorous acid (HOCl) and singlet oxygen ($^1O_2$) contributes to their strong antibacterial activity. These chemical species induce oxidative stress in bacterial cells, leading to antibacterial effects. AgNPs possess a high oxidation potential, which can result in lipid peroxidation, protein oxidative carbonylation, DNA/RNA strand breakage, and membrane structure damage. Additionally, AgNPs can denature cellular ribosomes, thereby inhibiting translation and protein synthesis. In addition, Ahmad et al. [68] reported that AgNPs inhibit respiratory chain enzymes and disrupt bacterial cell division. Previous studies have shown that Ag^+ ions released from AgNPs interact with the thiol group (-SH) in bacterial proteins, compromising their structural integrity and function, as well as interfering with DNA replication [68, 69]. Interestingly, AgNps can effectively target biofilms as both AgNPs and their released Ag^+ ions can penetrate extracellular polymeric substances. They interact with various biofilm components, disrupting bacterial metabolism and other vital cellular functions [70].

5. Conclusions

The methanolic leaf extract of *S. caseolaris* biosynthesised stable, polydisperse and near-spherical SC-AgNPs with an average size of 22.3 nm. SC-AgNPs demonstrated significant antibacterial activity against 12 *E. tarda* isolates including the β-haemolytic strain. The present findings suggest the potential of SC-AgNPs as an alternative therapeutic agent to antibiotics for the treatment of edwardsiellosis.

Funding
This research was supported by Exploratory Research Grant Scheme (ERGS), 1/2012 (ERGS/1/2012/STWN03/UMT/02/1) and Niche Research Grant Scheme (NRGS), NRGS/2014/53131/10, Ministry of Higher Education (MOHE), Malaysia. We are truly grateful for the MOHE MyPhD scholarship support for the doctorate study of the first author.

Authors Contribution
Alia Syafiqah Aznan: writing – original draft preparation, investigation, formal analysis, Kok Leong Lee: writing – review and editing, validation, methodology, formal analysis, Wan Nurhafizah Wan Ibrahim, Nur Azna Saari, Mohamad Tajuddin Abdul Manaf, Norhidayah Mohd Ahyat: investigation, Ruhil Hayati Hamdan: writing – review and editing, Musa Nadirah: conceptualisation, formal analysis, Yeong Yik Sung: conceptualisation, writing – review and editing, Alyza Azzura Abd Rahman Azmi: conceptualisation, writing – review and editing, Faizah Shaharom-Harrison: funding acquisition, Rossita Shapawi: writing – review and editing, Houjun Pan: writing – review and editing , Musa Najiah: conceptualisation, supervision, funding acquisition, writing – review and editing.

Availability of data and materials
The data that support the findings of this study are available from the corresponding author, upon reasonable request.

Conflict of interests
The authors declare that they have no known competing financial interests or personal relationships that could have appeared to influence the work reported in this paper.

References

[1] N. Bujan, H. Mohammed, S. Balboa, J.L. Romalde, A.E. Toranzo, and C.R. Arias. Genetic studies to re-affiliate *Edwardsiella tarda* fish isolates to *Edwardsiella piscicida* and *Edwardsiella anguillarum* species. *Syst. Appl. Microbiol.*, **41**:30–7, (2018).
DOI: https://doi.org/10.1016/j.syapm.2017.09.004.

[2] M.Y. Davies, de Oliveira M.G. Xavier, Vieira Cunha M. Paulo, et al. *Edwardsiella tarda* outbreak affecting fish and aquatic birds in Brazil. *Veterinary Quarterly*, **38**(1):99–105, (2018).
DOI: https://doi.org/10.1080/01652176.2018.1540070.

[3] L. An, J.L. Chan, M. Nguyen, S. Yang, and J.G. Deville. Case Report: Disseminated *Edwardsiella tarda* infection in an immunocompromised patient. *Front. Cell. Infect. Microbiol.*, **13**:1292768, (2023).
DOI: https://doi.org/10.3389/fcimb.2023.1292768.

[4] F. Hoque, P. Nilambari, P. Pranali, D. Rajdeep, et al. Pathogenesis and expression profile of selected immune genes to experimental *Edwardsiella tarda* infection in iridescent shark *Pangasianodon hypophthalmus*. *Aquaculture Reports*, **17**:100371, (2020).
DOI: https://doi.org/10.1016/j.aqrep.2020.100371.

[5] W. Rediet, S. Jirata, H. Yacob, and F. Abdi. Characterization of lesions in diseased fishes, isolation and identification of *Edwardsiella Tarda* from selected lakes and ponds of Ethiopia. *Am J Biomed Sci & Res.*, **17**(1), (2022).
DOI: https://doi.org/10.34297/AJBSR.2022.17.002301.

[6] T.P. Loch, J.P. Hawke, S.R. Reichley, M. Faisal, Piero F. Del, and M.J. Griffin. Outbreaks of edwardsiellosis caused by *Edwardsiella piscicida* and *Edwardsiella tarda* in farmed barramundi (*Lates calcarifer*). *Aquaculture*, **481**:202–210, (2017).
DOI: https://doi.org/10.1016/j.aquaculture.2017.09.005.

[7] W.J. Jung, J. Kwon, S.S. Giri, S.G. Kim, et al. Isolation and characterization of a highly virulent *Edwardsiella piscicida* strain responsible for mass mortality in marbled eel (*Anguilla marmorata*) cultured in Korea. *Aquaculture*, **555**:738199, (2022).
DOI: https://doi.org/10.1016/j.aquaculture.2022.738199.

[8] S.B. Fogelson, B.D. Petty, S.R. Reichley, et al. Histologic and molecular characterization of *Edwardsiella piscicida* infection in largemouth bass (*Micropterus salmoides*). *J. Vet. Diagn. Investig.*, **28**:338–344, (2016).
DOI: https://doi.org/10.1177/1040638716637639.

[9] M.Y. Elgendy, H. Ahmed, A.M. Sherif, et al. Phenotypic and molecular characterization of the causative agents of edwardsiellosis causing Nile tilapia (*Oreochromis niloticus*) summer mortalities. *Microbial Pathogenesis*, **169**, (2022).
DOI: https://doi.org/10.1016/j.micpath.2022.105620.

[10] S.B. Park, S.W. Nho, H.B. Jang, et al. Phenotypic and genotypic analysis of *Edwardsiella tarda* isolated from olive founder (*Paralichthys olivaceus)* and Japanese eel (*Anguilla japonica)*. *Aquaculture*, **473**: 449–455, (2017).
DOI: https://doi.org/10.1016/j.aquaculture.2017.03.015.

[11] V. Pandey, Bhat R.A. Hussain, S. Chandra, R.S. Tandel, et al. Clinical signs, lethal dose and histopathological lesions in grass carp, *Ctenopharyngodon idella* experimentally infected with *Edwardsiella tarda*. *Microb Pathog*, **161**:105292, (2021).
DOI: https://doi.org/10.1016/j.micpath.2021.105292.

[12] Y.J. Kim, L.J. Jun, D.W. Lee, Y.J. Lee, et al. Antibiotic susceptibility of bacterial pathogens that infect Olive Flounder (*Paralichthys olivaceus)* cultivated in Korea. *International Journal of Environmental Research and Public Health*, **19**(13):8110, (2022).
DOI: https://doi.org/10.3390/ijerph19138110.

[13] N.I.A. Ismail, M.N.A. Amal, S. Shohaimi, et al. Association of water quality and bacteria presence in cage cultured red hybrid tilapia, Oreochromis niloticus x *O. mossambicus*. *Aquaculture Reports*, **4**: 57–65, (2016).
DOI: https://doi.org/10.1016/j.aqrep.2016.06.004.

[14] W.W.I. Nurhafizah, K.L. Lee, A.A.R. Laith, M. Nadirah, et al. Virulence properties and pathogenicity of multidrug-resistant *Vibrio harveyi* associated with luminescent vibriosis in Pacific white shrimp, *Penaeus vannamei*. . *Journal of Invertebrate Pathology*, **186**:107594, (2021).
DOI: https://doi.org/10.1016/j.jip.2021.107594.

[15] R. Hamouda and H.M. Hosny. Synthesis and biological characterization of silver nanoparticles derived from the cyanobacterium *Oscillatoria limnetica*. *Nature Research*, **9**:13071, (2019).
DOI: https://doi.org/10.1038/s41598-019-49444-y.

[16] M. Shaalan, M. Saleh, M. El-mahdy, and M. El-Matbouli. Nanoparticles as a promising antipathogen in fish medicine. *Nanomedicine:Nanotechnology, Biology, and Medicine*, **12**:701–710, (2017).
DOI: https://doi.org/10.1016/j.nano.2015.11.005.

[17] T. Bruna, F. Maldonado-Bravo, P. Jara, and N. Caro. Silver nanoparticles and their antibacterial applications. *Int J Mol Sci.*, **22**(13):7202, (2021).
DOI: https://doi.org/10.3390/ijms22137202.

[18] C. Ma, B. Liu, L. Du, W. Liu, Y. Zhu, T. Chen, and othets. Green Preparation and antibacterial activity evaluation of AgNPs-*Blumea Balsamifera* oil nanoemulsion. *Molecules*, **29**:2009, (2024).
DOI: https://doi.org/10.3390/molecules29092009.

[19] S. Abedini, S. Pourseyedi, J. Zolala, H. Mohammadi, and R. Abdolshahi. Green synthesis of superparamagnetic iron oxide and silver nanoparticles in *Satureja Hortensis* leave extract: Evaluation of antifungal effects on Botryosphaeriaceae species. *Curr. Microbiol.*, **81**: 149, (2024).
DOI: https://doi.org/10.1007/s00284-024-03647-3.

[20] M.J. Saadh. Silver nanoparticles inhibit Goatpox Virus Replication. *Arch. Virol.*, **168**:32, (2023).
DOI: https://doi.org/10.1007/s00705-022-05667-5.

[21] W. Chartarrayawadee, P. Charoensin, J. Saenma, T. Rin, et al. Self-dual Leonard pairs green synthesis and stabilization of silver there antibacterial Hance extract and their activity. *Green Process Syntheses*, **9**:107–118, (2020).
DOI: https://doi.org/10.1515/gps-2020-0012.

[22] K. Nahar, S. Aziz, M.S. Bashar, et al. Synthesis and characterization of silver nanoparticles from Cinnamomum tamala leaf extract and its antibacterial potential. *International Journal of Nano Dimension*, **11** (1):88–98, (2020). URL https://www.magiran.com/p2069971.

[23] M. Jalal, M.A. Ansari, M.A. Alzohairy, et al. Biosynthesis of silver nanoparticles from oropharyngeal *Candida glabrata* isolates and their antimicrobial activity against clinical strains of bacteria and fungi. . *Nanomaterials*, **8**:586, (2018).
DOI: https://doi.org/10.3390/nano8080586.

[24] Rowida E. Ibrahim, E. Gehad, Gh. I. Elshopakey, et al. Palliative role of colloidal silver nanoparticles synthetized by moringa against *Saprolegnia spp.* infection in Nile Tilapia: Biochemical, immuno-antioxidant response, gene expression, and histopathological investigation. *Aquaculture Reports*, **26**:101318, (2022).
DOI: https://doi.org/10.1016/j.aqrep.2022.101318.

[25] M. Naveed, B. Bukhari, T. Aziz, S. Zaib, et al. Green synthesis of silver nanoparticles using the plant extract of *Acer oblongifolium* and study of its antibacterial and antiproliferative activity via mathematical approaches. *Molecules*, **27**(13):4226, (2022).
DOI: https://doi.org/10.3390/molecules27134226.

[26] H. Erjaee, H. Rajaian, and S. Nazifi. Synthesis and characterization of novel silver nanoparticles using *Chamaemelum nobile* extract for antibacterial application. *Advances in Natural Sciences: Nanoscience and Nanotechnology*, **8**(2):025004, (2017).
DOI: https://doi.org/10.1088/2043-6254/aa690b.

[27] V. Abdi, I. Sourinejad, M. Yousefzadi, and Z. Ghasemi. Mangrove-mediated synthesis of silver nanoparticles using native *Avicennia marina* plant extract from southern Iran. . *Chemical Engineering Communications*, **205**(8):1069–1076, (2018).
DOI: https://doi.org/10.1080/00986445.2018.1431624.

[28] P. Halifah, R. Hartati, H. Yusminah, and A.R. Roshanida. Phytochemical screening and antimicrobial activity from sonneratia caseolaris fruit extract. *Materials Science Forum*, **967**:28–33, (2019).
DOI: https://doi.org/10.4028/www.scientific.net/MSF.967.28.

[29] D.V. Thuoc, N.N. Mai, L.T.V. Ha, et al. Evaluation of antibacterial, antioxidant and antiobese activities of the fruit juice of crabapple mangrove *Sonneratia caseolaris* (Linn.). . *International Journal of Agricultural Sciences and Natural Resources*, **5**(2):25–29, (2018).
URL http://www.aascit.org/journal/ijasnr.

[30] J.M.W. Wibawanti, S. Mulyani, A.M. Legowo, R. Hartanto, et al. Characteristics of inulin from mangrove apple (*Soneratia caseolaris*) with different extraction temperatures. *Food Research*, **5**(4):99–106, (2021).
DOI: https://doi.org/10.26656/fr.2017.5(4).662.

[31] M. Bakshi, S. Ghosh, and P. Chaudhuri. Green synthesis, characterization and antimicrobial potential of silver nanoparticles using three mangrove plants from Indian Sundarban. *BioNanoSci.*, **5**:162170, (2015).
DOI: https://doi.org/10.1007/s12668-015-0175-8.

[32] K.A. Audah, J. Ettin, J. Darmadi, N.N. Azizah, et al. Indonesian mangrove *Sonneratia caseolaris* leaves ethanol extract is a potential super antioxidant and anti methicillin resistant *Staphylococcus aureus* Drug. *Molecules*, **27**:8369, (2022).
DOI: https://doi.org/10.3390/molecules27238369.

[33] J. Sambrook and D.W. Russell. Molecular cloning : A laboratory manual. *Cold Spring Harbor Laboratory Press*, , (2001).

[34] A.F. Vargas-Madriz, A. Kuri-Garcia, H. Vargas-Madriz, J.L. Chavez-Servin, and Ayala-Tirado. Phenolic profile and antioxidant capacity of fruit *Averrhoa carambola* L.: A review. *Food Science and Technology*, **v42**:e69920, (2022).
DOI: https://doi.org/10.1590/fst.69920.

[35] V. Ravichandran, S. Vasanthi, S. Shalini, S.A. Ali Shah, and R. Harish. Green synthesis of silver nanoparticles using *Atrocarpus altilis* leaf extract and the study of their antimicrobial and antioxidant activity. *Materials Letters*, **180**:264–267, (2016).
DOI: https://doi.org/10.1016/j.matlet.2016.05.172.

[36] R. Krishnan, A. Vijay, and S.K. Vasaviah. The MIC and MBC of silver nanoparticles against *Enterococcus faecalis* - A facultative anaerobe. *Journal of Nanomedicine and Nanotechnology*, **6**(3):1–4, (2015).
DOI: https://doi.org/10.4172/2157-7439.1000285.

[37] S. Zhang, Y. Zou, Q. Guo, J. Chen, et al. AR-12 exhibits direct and host-targeted antibacterial activity toward *Mycobacterium abscessus*. Antimicrob. *Agents Chemother*, **64**:e00236–20, (2020).
DOI: https://doi.org/10.1128/AAC.00236-20.

[38] K.W. Goh, Z. Abdul Kari, W. Wee, N.N.A. Zakaria, et al. Exploring the roles of phytobiotics in relieving the impacts of *Edwardsiella tarda* infection on fish: a mini-review. *Front. Vet. Sci.*, **10**:1149514, (2023).
DOI: https://doi.org/10.3389/fvets.2023.1149514.

[39] O.D. Butar-Butar, D. Suryanto, and S. Ilyas. Detection of Edwardsiella tarda infection of catfish (*Clarias gariepinus*) in Central Tapanuli Regency, NorthSumatra, Indonesia. . *IOSR Journal of Agriculture and Veterinary Science*, **13**(1):6–13, (2020).
DOI: https://doi.org/10.9790/2380-1301020613.

[40] J.F. Zachary. Mechanisms of microbial infections. *Pathologic Basis of Veterinary Disease Expert Consult*, :132–241, (2017).
DOI: https://doi.org/10.1016/B978-0-323-35775-3.00004-7.

[41] T.C. Jackson, B.O. Patani, and N.N. Udosen. Surface plasmon resonance and antimicrobial properties of novel silver nanoparticles prepared from some indigenous plants in Uyo, Nigeria. *African Journal of Biotechnology*, **17**(24):748–752, (2018).
DOI: https://doi.org/10.5897/AJB2017.16119.

[42] S. Jain and M.S. Mehata. Medicinal plant leaf extract and pure flavonoid mediated green synthesis of silver nanoparticles and their enhanced antibacterial property. *Scientific Reports*, **7**(15867):1–13, (2017).
DOI: https://doi.org/10.1038/s41598-017-15724-8.

[43] G.M. Srirangam and K. Parameswara Rao. Synthesis and charcterization of silver nanoparticles from the leaf extract of *Malachra capitata (L.)*. . *Rasayan Journal of Chemistry*, **10**(1):46–53, (2017).
DOI: https://doi.org/10.7324/RJC.2017.1011548.

[44] R. Vijayaraj, G.D. Kumar, and N.S. Kumaran. In-vitro anti-inflammatory activity of silver nanoparticle synthesised *Avicennia marina (Forssk.) Vierh.* : A green synthetic approach. . *International Journal of Green Pharmacy*, **12**(3):S528–S536, (2018).
DOI: https://doi.org/10.22377/ijgp.v12i03.2014.

[45] A.K. Giri, B. Jena, B. Biswal, et al. Green synthesis and characterization of silver nanoparticles using *Eugenia roxburghii* DC. extract and activity against biofilm-producing bacteria. *Scientific Reports*, **12**:8383, (2022).
DOI: https://doi.org/10.1038/s41598-022-12484-y.

[46] El-Aziz D.M. Abd and N.M.H. Yousef. Enhancement of antimicrobial effect of some spices extract by using biosynthesised silver nanoparticles. *International Food Research Journal*, **25**(2):589–596, (2018). URL http://www.ifrj.upm.edu.my.

[47] M. Asif, R. Yasmin, R. Asif, A. Ambreen, M. Mustafa, and S. Umbreen. Green Synthesis of Silver Nanoparticles (AgNPs), Structural characterization, and their antibacterial potential. *Dose Response*, **20** (2):15593258221088709, (2022).
DOI: https://doi.org/10.1177/15593258221088709.

[48] O. Dlugosz, J. Chwastowski, and M. Banach. Hawthorn berries extract for the green synthesis of copper and silver nanoparticles. *Chemical Papers*, **74**:239–252, (2020).
DOI: https://doi.org/10.1007/s11696-019-00873-z.

[49] A. Dhaka, C.M. Suresh, S. Sheetal, and T. Rohini. A review on biological synthesis of silver nanoparticles and their potential applications. *Results in Chemistry*, **6**:101108, (2023).
DOI: https://doi.org/10.1016/j.rechem.2023.101108.

[50] S. Palithya, A.A. Gaddam, V.S. Kotakadi, et al. Green synthesis of silver nanoparticles using flower extracts of *Aerva lanata* and their biomedical applications. *Particulate Science and Technology*, **40**(1): 84–96, (2022).
DOI: https://doi.org/10.1080/02726351.2021.1919259.

[51] D.H. Nguyen, N.N.V. Thanh, T.T.L. Ngoc, et al. Evaluation of saponin-rich/poor leaf extract-mediated silver nanoparticles and their antifungal capacity. *Green Processing and synthesis*, **9**(1):429–439, (2020).
DOI: https://doi.org/10.1515/gps-2020-0044.

[52] H.R. El-seedi, R.M. El-shabasy, S.A.M. Khalifa, et al. Metal nanoparticles fabricated by green chemistry using natural extracts : Biosynthesis, mechanisms, and application. *RSC Advances*, **9**:24539–24559, (2019).
DOI: https://doi.org/10.1039/c9ra02225b.

[53] U. Jeyapaul, S. Parvathikrishnan, A.J. Bosco, S. Balasubramanian, and S.M.J. Kala. Biosynthesis of silver nanoparticles using *Triumfetta Rhomboidea* leaf extract and the anti-bacterial efficacy. . *International Journal of Advanced Chemical Science and Applications*, **3** (1):17–20, (2015).

[54] C. Yu, T. Jingchun, L. Xiaomei, R. Xinwei, Z. Meinan, and W. Lan. Green biosynthesis of silver nanoparticles using *Eriobotrya japonica* (Thunb.) leaf extract for reductive catalysis. *Materials*, **12**(1):189, (2019).
DOI: https://doi.org/10.3390/ma12010189.

[55] E.K. Kambale, I.N. Christian, and others Blaise-Pascal, I.M. Green synthesis of antimicrobial silver nanoparticles using aqueous leaf extracts from three Congolese plant species (*Brillantaisia patula*, *Crossopteryx febrifuga* and *Senna siamea*). . *Heliyon*, **6**(8):e04493, (2020).
DOI: https://doi.org/10.1016/j.heliyon.2020.e04493.

[56] B. Das, S.K. Dash, D. Mandal, T. Ghosh, S. Chattopadhay, S. Tripathy, S. Das, S.K. Dey, D. Das, and S. Roy. Green synthesised silver nanoparticles destroy multidrug resistant bacteria via reactive oxygen species mediated membrane damage. *Arabian Journal of Chemistry*, **10**:862–876, (2017).
DOI: https://doi.org/10.1016/j.arabjc.2015.08.008.

[57] A.R. Hassan and D.E. Mustafa. Green synthesis of silver nanoparticles mediated by traditionally used medicinal plants in Sudan. *International Nano Letters*, **10**:1–14, (2020).
DOI: https://doi.org/10.1007/s40089-019-00291-9.

[58] M.A. Higo, A.E. Ranwa, T. Hekmate, E. Fatma, and M.T. Hend. Green synthesis and characterization of silver nanoparticles using *Bauhinia variegate* leaves aqueous extract. . *Biomedical Journal of Scientific & Technical Research*, **29**(5):22803–22808, (2020).
DOI: https://doi.org/10.26717/BJSTR.2020.29.004862.

[59] B. Khalandi, N. Asadi, M. Milani, S. Davaran, et al. A review on potential role of silver nanoparticles and possible mechanisms of their actions on bacteria. *Drug Res (Stuttg)*, **67**(2):70–76, (2017).
DOI: https://doi.org/10.1055/s-0042-113383.

[60] T.C. Dakal, A. Kumar, R.S. Majumdar, and V. Yadav. Mechanistic basis of antimicrobial actions of silver nanoparticles. *Frontiers in Microbiology*, **7**:1–17, (2016).
DOI: https://doi.org/10.3389/fmicb.2016.01831.

[61] D.M. Ibrahim, H.M. Idris, and H.M. Mohammed. Comparison between green and chemical synthesis of silver nanoparticles : Characterization and antibacterial activity. . *Al-Muhktar Journal of Basic Sciences*, **22**(2):103–113, (2024).
DOI: https://doi.org/10.54172/0xd07091.

[62] S. Bahraminezhad, M.R. Mehrasbi, P. Homauoni, and Z. Farahmandkia. A Comparative analysis of the antibacterial effects of green-synthesized silver nanoparticles with chemically synthesized silver nanoparticles. *Journal of Human Environment and Health Promotion*, **11**(3):175–181, (2025).
DOI: https://doi.org/10.61186/jhehp.11.3.175.

[63] S.K. Salahuddin, H. Azamal, and A.K.R. Rifaqat. A review on biosynthesis of silver nanoparticles and their biocidal properties. *Journal of Nanobiotechnology*, **16**(14):1–28, (2018).
DOI: https://doi.org/10.1186/s12951-018-0334-5.

[64] P.R. More, S. Pandit, A.D. Filippis, G. Franci, I. Mijakovic, and M. Galdiero. Silver Nanoparticles: Bactericidal and mechanistic approach against drug resistant pathogens. . *Microorganisms*, **11**: 369, (2023).
DOI: https://doi.org/10.3390/microorganisms11020369.

[65] A. Roy, B. Onur, S. Sudip, K.M. Amit, and Y.M. Deniz. Green synthesis of silver nanoparticle: Biomolecule-nanoparticle organizations targeting antimicrobial activity. . *RSC Advances*, **9**:2673–2702, (2019).
DOI: https://doi.org/10.1039/C8RA08982E.

[66] K.S. Siddiqi, A. Husen, and R.A.K. Rao. A review on biosynthesis of silver nanoparticles and their biocidal properties. . *J Nanobiotechnol*, **16**:16, (2018).
DOI: https://doi.org/10.1186/s12951-018-0334-5.

[67] A. Girma, G. Alamnie, T. Bekele, G. Mebratie, B. Mekuye, et al. Green synthesised silver nanoparticles: antibacterial activity and alternative mechanisms of action to combat multidrug-resistant bacterial pathogens: a systematic literature review. . *Green Chemistry Letters and Reviews*, **17**(1):2412601, (2024).
DOI: https://doi.org/10.1080/17518253.2024.2412601.

[68] S.A. Ahmad, S.S. Das, A. Khatoon, et al. Bactericidal activity of silver nanoparticles: A mechanistic review. *Materials Science for Energy Technologies*, **3**:756–769, (2020).
DOI: https://doi.org/10.1016/j.mset.2020.09.002.

[69] X. Jiang, S. Khan, A. Dykes, E. Stulz, and X. Zhang. Biogenic Synthesis of Silver Nanoparticles and Their Diverse Biomedical Applications. . *Molecules*, **30**(15):3104, (2025).
DOI: https://doi.org/10.3390/molecules30153104.

[70] M.V. Zykova, M.R. Karpova, Y. Zhang, et al. The Influence of Silver-Containing Bionanomaterials Based on Humic Ligands on Biofilm Formation in Opportunistic Pathogens. *Nanomaterials*, **14**: 1453, (2024).
DOI: https://doi.org/10.3390/nano14171453.